



# Crystal structures and magnetic behaviour of new complex lanthanide chlorides with organic cations

Annette Becker, Werner Urland\*

*Institut für Anorganische und Analytische Chemie der Universität Hannover, Callinstraße 9, 30167 Hannover, Germany*

## Abstract

Crystal structures of the new complex lanthanide chlorides with organic cations  $[(\text{CH}_3)_2\text{NH}_2]_4[\text{LnCl}_6]\text{Cl}$  ( $\text{Ln}=\text{Ho}-\text{Tm}$ ) have been determined. The air sensitive compounds have been prepared by the reaction of  $\text{LnCl}_3 \cdot x\text{H}_2\text{O}$  with  $[(\text{CH}_3)_2\text{NH}_2]\text{Cl}$  in ethanol/butanol. The complex chlorides are isotypic with each other and crystallize in the orthorhombic space group  $P2_12_12$  ( $Z=2$ ). The magnetic behaviour of these complex lanthanide chlorides has been studied. The magnetic data were interpreted by ligand field calculations applying the angular overlap model. © 1998 Elsevier Science S.A.

**Keywords:** Complex lanthanide chlorides; Preparation; Crystal structure; Magnetic behaviour

## 1. Introduction

There are several publications on complex (water containing) lanthanide chlorides with organic cations being of structural and magnetic interest [1–6]. Here we present the crystal structures of the new complex chlorides  $[(\text{CH}_3)_2\text{NH}_2]_4[\text{LnCl}_6]\text{Cl}$  ( $\text{Ln}=\text{Ho}-\text{Tm}$ ), containing isolated  $[\text{LnCl}_6]^{3-}$  units. In order to study the interactions between lanthanide and chloride ions we also investigated the magnetic behaviour of  $[(\text{CH}_3)_2\text{NH}_2]_4[\text{LnCl}_6]\text{Cl}$  ( $\text{Ln}=\text{Ho}-\text{Tm}$ ). The magnetic data were interpreted by ligand field calculations applying the angular overlap model [7,8].

## 2. Experimental details

### 2.1. Synthesis

The compounds have been obtained by the reaction of  $\text{LnCl}_3 \cdot 6\text{H}_2\text{O}$  ( $\text{Ln}=\text{Ho}-\text{Tm}$ ) (Strem Chemicals, 99.9%) with dimethylamine hydrochloride ( $[(\text{CH}_3)_2\text{NH}_2]\text{Cl}$ ) (Aldrich, 99%) (molar ratio 1:3) in an ethanol (Sigma Aldrich, denaturated HPLC grade)/butanol (Aldrich, 99%) mixture. The transparent crystals of the compounds (Ho: salmon-

pink, Er: pink, Tm: colourless) form small cubes and are sensitive to moisture.

### 2.2. Data collection and structure determination

In the case of  $[(\text{CH}_3)_2\text{NH}_2]_4[\text{ErCl}_6]\text{Cl}$ , X-ray intensity measurements for crystal structure solution were performed at room temperature on a four-circle diffractometer (SIEMENS-STOE, AED). For  $[(\text{CH}_3)_2\text{NH}_2]_4[\text{LnCl}_6]\text{Cl}$  ( $\text{Ln}=\text{Ho}, \text{Tm}$ ) data collection was carried out at room temperature with an 'Imaging Plate' diffractometer (STOE, IPDS). The fundamental measurement and refinement data are summarized in Table 1.

### 2.3. Magnetic measurements

Magnetic susceptibility measurements on crushed single crystals of the complex chlorides were performed with a SQUID magnetometer (Quantum Design, MPMS 5) in the 1.7–300 K temperature range at field strengths of 1–10 kOe. The magnetic susceptibilities were corrected for diamagnetism [9]. The susceptibilities are practically independent of the magnetic field.

## 3. Results and discussion

The compounds  $[(\text{CH}_3)_2\text{NH}_2]_4[\text{LnCl}_6]\text{Cl}$  ( $\text{Ln}=\text{Ho}-\text{Tm}$ )

\*Corresponding author.

Table 1

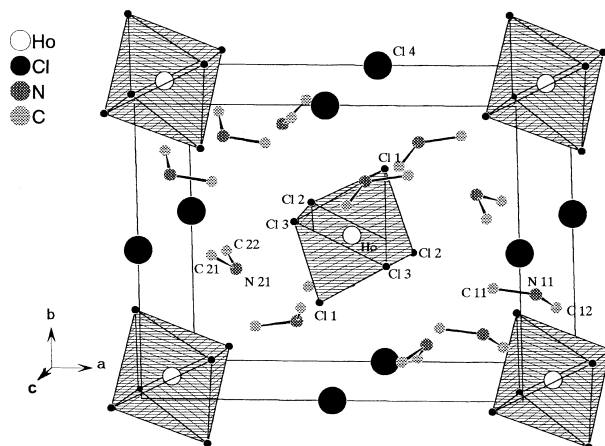
Crystal and refinement data for  $[(\text{CH}_3)_2\text{NH}_2]_4[\text{LnCl}_6]\text{Cl}$  (Ln=Ho–Tm)

	$[(\text{CH}_3)_2\text{NH}_2]_4[\text{HoCl}_6]\text{Cl}$	$[(\text{CH}_3)_2\text{NH}_2]_4[\text{ErCl}_6]\text{Cl}$	$[(\text{CH}_3)_2\text{NH}_2]_4[\text{TmCl}_6]\text{Cl}$
Cell parameters (293 K) (pm)	$a=1329.7(2)$ $b=1032.2(1)$ $c=876.4(2)$	$a=1326.5(1)$ $b=1033.5(1)$ $c=876.4(1)$	$a=1325.0(2)$ $b=1032.5(1)$ $c=876.1(1)$
Space group, $Z$	$P2_12_12_1$ , 2	$P2_12_12_1$ , 2	$P2_12_12_1$ , 2
$\rho$ (X-ray) ( $\text{g cm}^{-3}$ )	1.560	1.569	1.577
Crystal dimensions ( $\text{mm}^3$ )	$0.184 \times 0.222 \times 0.148$	$0.152 \times 0.152 \times 0.114$	$0.190 \times 0.222 \times 0.158$
Diffractometer	STOE, IPDS	SIEMENS STOE, (AED-2)	STOE, IPDS
Radiation (pm)	Mo $K\alpha$ ( $\lambda=71.073$ )	Mo $K\alpha$ ( $\lambda=71.073$ )	Mo $K\alpha$ ( $\lambda=71.073$ )
$R_{\text{int}}$	4.25%	5.45%	9.58%
Absorption correction	Numerical [11]	Empirical	None
$2\theta$ range	$4.6^\circ \leq 2\theta \leq 56.2^\circ$	$4.6^\circ \leq 2\theta \leq 52.1^\circ$	$4.6^\circ \leq 2\theta \leq 56.6^\circ$
$h, k, l$ range	$\pm 17, \pm 13, \pm 11$	$\pm 16, \pm 12, \pm 10$	$\pm 17, \pm 13, \pm 11$
Standard reflections	-	$-9\ 1\ 0, -9\ -1\ 0, 5\ 2\ -4, -5\ 2\ 4$	-
No. of observed reflections	12936	5067	13150
No. of unique reflections	2895	2379	2937
Linear absorption factor ( $\text{cm}^{-1}$ )	40.6	42.6	44.7
Refined parameters	93 <sup>a</sup>	93 <sup>a</sup>	93 <sup>a</sup>
Refinement	Full-matrix least-squares, based on $F^2$	Full-matrix least-squares, based on $F^2$	Full-matrix least-squares, based on $F^2$
$R1^b, wR2^b$	2.72%, 5.25% (no $\sigma$ limit)	7.06%, 9.23% (no $\sigma$ limit)	6.66%, 7.28% (no $\sigma$ limit)
$\text{Goof}=\text{S}^b$	1.052	1.029	0.909
Min., max. $\Delta\rho$ ( $\text{e pm}^{-3} \times 10^{-6}$ )	-0.41, 0.45	-1.03, 2.07	-1.41, 0.65
Programs used	SHELXS(86) [12], SHELXL(93) [13], Stoe IPDS software <sup>c</sup> [14]	SHELXS(86) [12], SHELXL(93) [13], STRUCSY <sup>c</sup> [15]	SHELXS(86) [12], SHELXL(93) [13], Stoe IPDS software <sup>c</sup> [14]

<sup>a</sup> Including extinction coefficient.<sup>b</sup> Definition given in [13].<sup>c</sup> Data reduction and intensity correction.

are isotopic with each other and crystallize in the orthorhombic space group  $P2_12_12_1$ ,  $Z=2$ . The positional and displacement parameters are given in Table 2.<sup>1</sup> The structure of  $[(\text{CH}_3)_2\text{NH}_2]_4[\text{HoCl}_6]\text{Cl}$  is shown in Fig. 1. Basic structural units are slightly distorted isolated  $[\text{HoCl}_6]^{3-}$ -octahedra, which are interconnected via Cl...N hydrogen bonds [10] with  $[(\text{CH}_3)_2\text{NH}_2]^+$  cations forming anionic  $[(\text{CH}_3)_2\text{NH}_2]_2(\text{HoCl}_6)^-$  layers in the  $ab$ -plane (Fig. 2). Isolated chloride ions, each of them linked via Cl...N hydrogen bonds [10] with two further  $[(\text{CH}_3)_2\text{NH}_2]^+$  cations, built up  $[(\text{CH}_3)_2\text{NH}_2]_2\text{Cl}^+$  units lying in layers (Fig. 3), which are alternately stacked with the above mentioned anionic layers along  $[001]$  (Fig. 4). In Fig. 5 the observed reciprocal magnetic susceptibilities for  $[(\text{CH}_3)_2\text{NH}_2]_4[\text{HoCl}_6]\text{Cl}$  (■),  $[(\text{CH}_3)_2\text{NH}_2]_4[\text{ErCl}_6]\text{Cl}$  (×) and  $[(\text{CH}_3)_2\text{NH}_2]_4[\text{TmCl}_6]\text{Cl}$  (▲) at a field strength of  $H=1000$  Oe are shown. At low temperatures the

magnetism of the holmium and thulium compounds shows temperature independent behaviour. In order to interpret the measured susceptibilities we carried out ligand field calculations applying the angular overlap model [7,8], using the parameters  $F_2, F_4, F_6$  (electrostatic interaction)

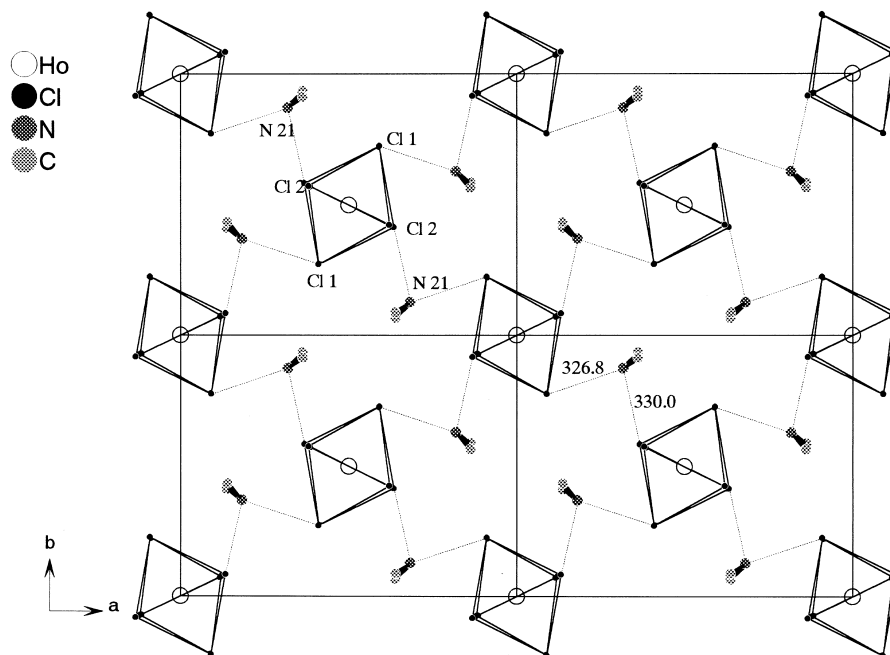
Fig. 1. Unit cell of  $[(\text{CH}_3)_2\text{NH}_2]_4[\text{HoCl}_6]\text{Cl}$ .

<sup>1</sup> Further details of the crystal structure investigations can be requested at the FACHINFORMATIONSZENTRUM KARLSRUHE, 76344 Eggenstein-Leopoldshafen 2 by giving the deposit numbers: CSD 407 710  $[(\text{CH}_3)_2\text{NH}_2]_4[\text{HoCl}_6]\text{Cl}$ , CSD 407 712  $[(\text{CH}_3)_2\text{NH}_2]_4[\text{ErCl}_6]\text{Cl}$ , CSD 407 711  $[(\text{CH}_3)_2\text{NH}_2]_4[\text{TmCl}_6]\text{Cl}$ .

Table 2

Site multiplicities, fractional atomic coordinates, and equivalent displacement parameters ( $\text{pm}^2$ ) for  $[(\text{CH}_3)_2\text{NH}_2]_4[\text{LnCl}_6]\text{Cl}$  (Ln=Ho–Tm)

Atom	Site	$x/a$	$y/b$	$z/c$	$U_{\text{eq}}^a$
Ho	2a	0	0	0.43031(2)	296(1)
Cl1	4c	-0.0904(1)	0.2263(1)	0.4367(1)	468(2)
Cl2	4c	0.1329(1)	0.0842(1)	0.6281(1)	452(2)
Cl3	4c	0.1202(1)	0.0751(1)	0.2110(2)	675(3)
Cl4	2b	0	0.5	-0.0071(3)	1104(8)
N11	4c	-0.0945(3)	0.2357(4)	0.0398(4)	516(9)
N21	4c	-0.3177(3)	0.1285(5)	0.5193(6)	742(14)
C11	4c	-0.2055(4)	0.2562(6)	0.0543(8)	825(17)
C12	4c	-0.0628(6)	0.1724(6)	-0.1062(7)	963(22)
C21	4c	-0.3620(5)	0.0653(6)	0.3830(8)	818(17)
C22	4c	-0.3623(4)	0.0878(5)	0.6641(7)	713(15)
Er	2a	0	0	0.42984(6)	322(2)
Cl1	4c	0.0901(2)	0.2256(2)	0.4364(4)	485(6)
Cl2	4c	-0.1324(2)	0.0839(2)	0.6277(3)	466(6)
Cl3	4c	-0.1199(2)	0.0752(3)	0.2116(3)	675(8)
Cl4	2b	0	0.5	-0.0078(6)	1138(19)
N11	4c	0.0935(6)	0.2339(8)	0.0390(9)	518(22)
N21	4c	-0.3178(6)	-0.1281(10)	0.5217(14)	793(36)
C11	4c	0.2047(9)	0.2595(14)	0.0589(19)	863(40)
C12	4c	0.0620(11)	0.1699(12)	-0.1039(16)	925(46)
C21	4c	-0.3613(10)	-0.0633(13)	0.3864(16)	800(38)
C22	4c	-0.3608(8)	-0.0894(12)	0.6671(16)	764(38)
Tm	2a	0	0	0.42964(4)	327(1)
Cl1	4c	-0.0895(1)	0.2250(1)	0.4356(3)	482(4)
Cl2	4c	0.1320(1)	0.0834(2)	0.6264(2)	471(4)
Cl3	4c	0.1198(2)	0.0754(2)	0.2134(2)	663(6)
Cl4	2b	0	0.5	-0.0088(4)	1105(13)
N11	4c	-0.0944(5)	0.2355(6)	0.0399(6)	538(16)
N21	4c	-0.3181(5)	0.1306(8)	0.5212(9)	754(23)
C11	4c	-0.2053(7)	0.2587(10)	0.0547(13)	821(27)
C12	4c	-0.0618(9)	0.1705(11)	-0.1052(10)	981(35)
C21	4c	-0.3614(8)	0.0641(9)	0.3873(11)	799(28)
C22	4c	-0.3613(7)	0.0866(9)	0.6661(11)	757(26)

<sup>a</sup>  $U_{\text{eq}} = 1/3 (U_{11} + U_{22} + U_{33})$  [16].Fig. 2.  $[(\text{CH}_3)_2\text{NH}_2]_2(\text{HoCl}_6)^-$  layers in  $[(\text{CH}_3)_2\text{NH}_2]_4[\text{HoCl}_6]\text{Cl}$  projected down  $c$ . Hydrogen bonds are indicated by dotted lines.

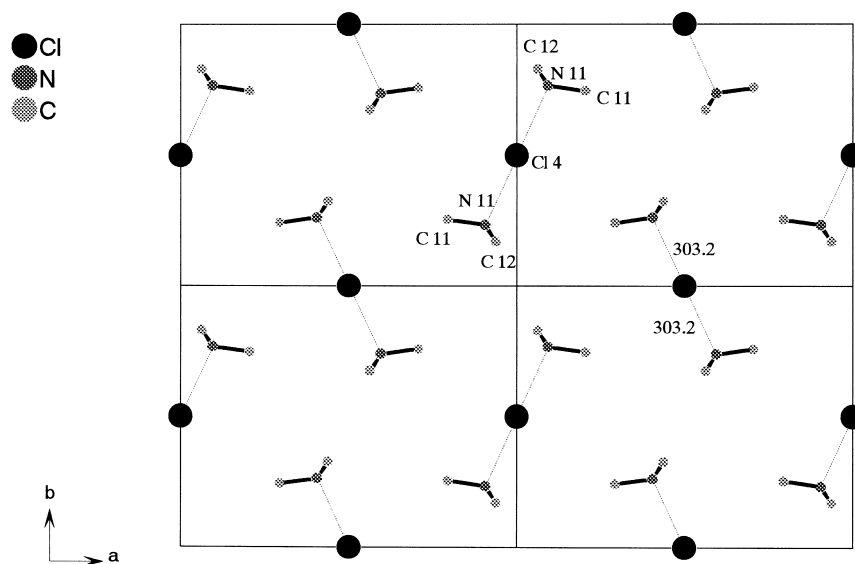


Fig. 3. Layers containing  $[(\text{CH}_3)_2\text{NH}_2]_2\text{Cl}^+$  units in  $[(\text{CH}_3)_2\text{NH}_2]_4[\text{HoCl}_6]\text{Cl}$  projected down  $c$ . Hydrogen bonds are indicated by dotted lines.

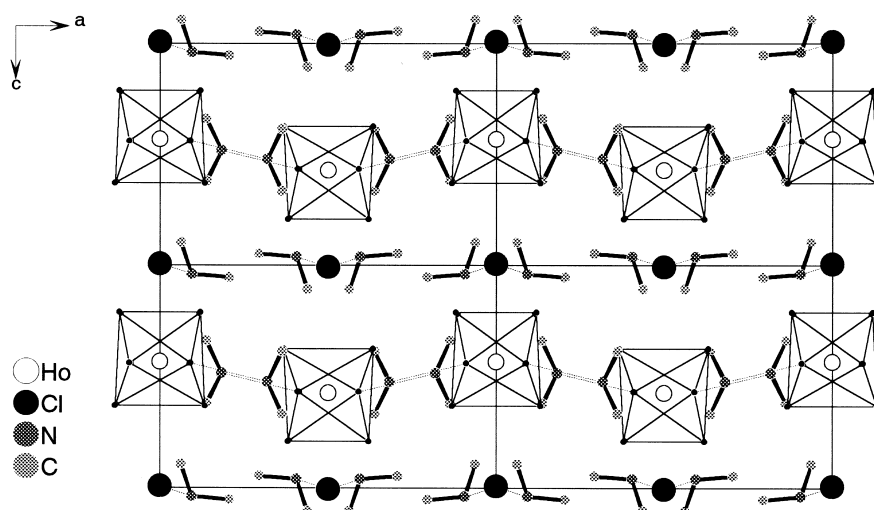


Fig. 4. Projection of the crystal structure of  $[(\text{CH}_3)_2\text{NH}_2]_4[\text{HoCl}_6]\text{Cl}$  on (010). Hydrogen bonds are indicated by dotted lines.

and  $\zeta$  (spin orbit coupling) (Table 3) [17–19]. The angular overlap parameters  $e_\sigma$  and  $e_\pi$  (Table 3) representing  $\sigma$ - and  $\pi$ -bonding between lanthanide and chloride ions were obtained by fitting procedures using the spiral algorithm of Jones [20]. In Fig. 5 the good agreement of the observed ( $\blacksquare$ ,  $\times$ ,  $\blacktriangle$ ) and calculated (fitted) (—) susceptibilities of the complex chlorides are shown. The derived  $e_\sigma$  values decrease along the lanthanide series, the  $e_\sigma/e_\pi$  ratios are constant at  $3.0 \pm 0.2$  (cf. Table 3). The  $e_\sigma$  and  $e_\pi$  values are in line with those found for octahedral  $[\text{LnCl}_6]^{3-}$  units in  $\text{Cs}_2\text{KTmCl}_6$  ( $e_\sigma = 210 \text{ cm}^{-1}$ ,  $e_\sigma/e_\pi = 3$ ) [21] and  $\text{Cs}_2\text{NaHoCl}_6$  ( $e_\sigma = 307 \text{ cm}^{-1}$ ,  $e_\sigma/e_\pi = 2.2$ ) [22].

Table 3  
Angular overlap parameters  $e_\sigma$  ( $\text{cm}^{-1}$ ) and  $e_\pi$  ( $\text{cm}^{-1}$ ) for  $[(\text{CH}_3)_2\text{NH}_2]_4[\text{LnCl}_6]\text{Cl}$  ( $\text{Ln} = \text{Ho} - \text{Tm}$ )

	$\text{Ln} = \text{Ho}^a$	$\text{Ln} = \text{Er}^b$	$\text{Ln} = \text{Tm}^c$
$e_\sigma$	249	243	208
$e_\pi$	83	78	74
$e_\sigma/e_\pi$	3.0	3.1	2.8

<sup>a</sup>  $\text{Ho}^{3+}$ : basis set  $^5\text{I}$ ;  $\zeta = 2163 \text{ cm}^{-1}$  [17].

<sup>b</sup>  $\text{Er}^{3+}$ : basis set  $^4\text{S}$ ,  $^4\text{D}$ ,  $^4\text{F}$ ,  $^4\text{G}$ ,  $^4\text{I}$ ,  $^2\text{P}$ ,  $^2\text{D}(1)$ ,  $^2\text{D}(2)$ ,  $^2\text{F}(1)$ ,  $^2\text{F}(2)$ ,  $^2\text{G}(1)$ ,  $^2\text{G}(2)$ ,  $^2\text{H}(1)$ ,  $^2\text{H}(2)$ ,  $^2\text{I}$ ,  $^2\text{K}$ ,  $^2\text{L}$ ;  $F_2 = 433.200 \text{ cm}^{-1}$ ,  $F_4 = 67.130 \text{ cm}^{-1}$ ,  $F_6 = 7.356 \text{ cm}^{-1}$ ,  $\zeta = 2393.3 \text{ cm}^{-1}$  [18].

<sup>c</sup>  $\text{Tm}^{3+}$ : basis set  $^3\text{P}$ ,  $^3\text{F}$ ,  $^3\text{H}$ ,  $^1\text{S}$ ,  $^1\text{D}$ ,  $^1\text{G}$ ,  $^1\text{I}$ ;  $F_2 = 446.70 \text{ cm}^{-1}$ ,  $F_4 = 70.491 \text{ cm}^{-1}$ ,  $F_6 = 7.534 \text{ cm}^{-1}$ ,  $\zeta = 2617 \text{ cm}^{-1}$  [19].

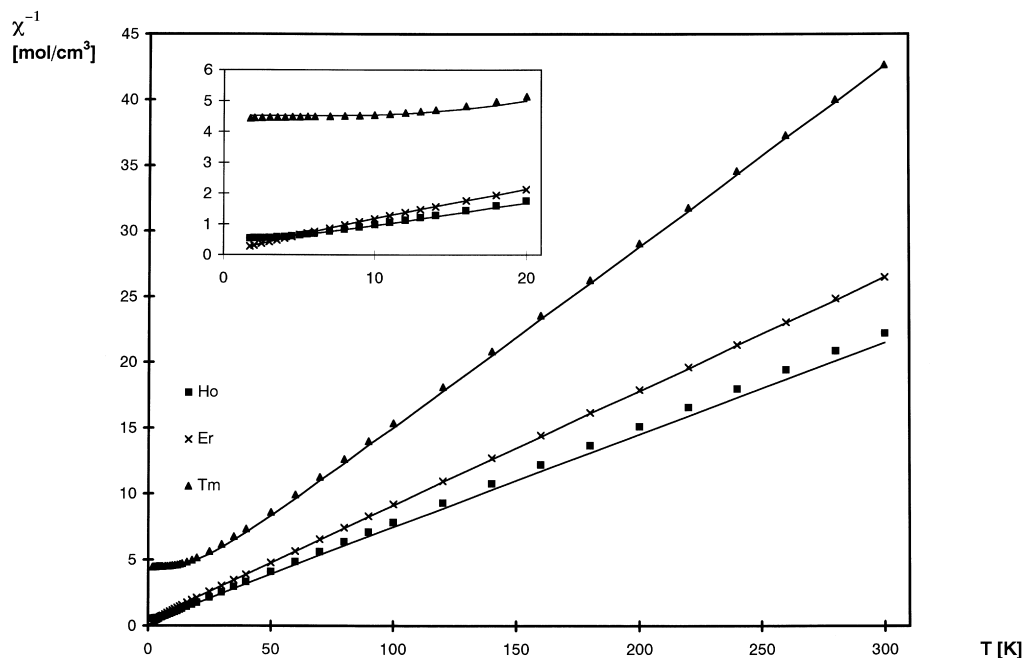


Fig. 5. Comparison of measured (■, ×, ▲) and calculated (—) inverse magnetic susceptibilities for  $[(\text{CH}_3)_2\text{NH}_2]_4[\text{HoCl}_6]\text{Cl}$  (■),  $[(\text{CH}_3)_2\text{NH}_2]_4[\text{ErCl}_6]\text{Cl}$  (×) and  $[(\text{CH}_3)_2\text{NH}_2]_4[\text{TmCl}_6]\text{Cl}$  (▲).

## References

- [1] P. Runge, M. Schulze, W. Urland, *Z. Naturforsch.* 45b (1990) 603.
- [2] P. Runge, M. Schulze, W. Urland, *Z. Anorg. Allg. Chem.* 592 (1991) 115.
- [3] M. Czjzek, H. Fuess, I. Pabst, *Z. Anorg. Allg. Chem.* 617 (1992) 105.
- [4] D. Mackenstedt, W. Urland, *Z. Anorg. Allg. Chem.* 619 (1993) 893.
- [5] D. Mackenstedt, W. Urland, *Z. Anorg. Allg. Chem.* 619 (1993) 1393.
- [6] D. Mackenstedt, W. Urland, *J. Alloys Comp.* 207–208 (1994) 189.
- [7] W. Urland, *Chem. Phys.* 14 (1976) 393.
- [8] W. Urland, *Chem. Phys. Lett.* 46 (1977) 457.
- [9] P.W. Selwood, *Magnetochemistry*, 2nd ed., Interscience Publishers, New York, 1956.
- [10] A.F. Wells, *Structural Inorganic Chemistry*, 5th ed., Clarendon Press, Oxford, 1986, p. 357.
- [11] STOE, X-SHAPE, Crystal Optimisation for Numerical Absorption Correction, Rev. 1.01, 1996.
- [12] G.M. Sheldrick, SHELXS-86 Program for Crystal Structure Determination, Universität Göttingen, 1986.
- [13] G.M. Sheldrick, SHELXL-93, A Program for Crystal Structure Refinement, Universität Göttingen, 1993.
- [14] STOE, IPDS Software, Darmstadt.
- [15] SIEMENS-STOE, STRUCSY, Program Package for Crystal Structure Solution, Darmstadt.
- [16] R.X. Fischer, E. Tillmanns, *Acta Crystallogr.* C44 (1988) 775.
- [17] M.H. Crozier, W.A. Runciman, *J. Chem. Phys.* 35 (1961) 1392.
- [18] J.C. Eisenstein, *J. Chem. Phys.* 39 (1963) 2128.
- [19] J.B. Gruber, W.F. Krupke, J.M. Poindexter, *J. Chem Phys.* 41 (1964) 3363.
- [20] A. Jones, *Comp. J.* 13 (1970) 301.
- [21] W. Urland, *Ber. Bunsenges. Phys. Chem.* 83 (1979) 1042.
- [22] W. Urland, *Chem. Phys. Lett.* 83 (1981) 116.